

Epitaxial growth and demonstration of hexagonal BN/AlGaN p-n junctions for deep ultraviolet photonics

S. Majety, J. Li, X. K. Cao, R. Dahal, B. N. Pantha et al.

Citation: *Appl. Phys. Lett.* **100**, 061121 (2012); doi: 10.1063/1.3682523

View online: <http://dx.doi.org/10.1063/1.3682523>

View Table of Contents: <http://apl.aip.org/resource/1/APPLAB/v100/i6>

Published by the [American Institute of Physics](#).

Related Articles

Structure and chemistry of the Si(111)/AlN interface

Appl. Phys. Lett. **100**, 011910 (2012)

Catalyst-free growth of high-optical quality GaN nanowires by metal-organic vapor phase epitaxy

Appl. Phys. Lett. **99**, 251910 (2011)

High temperature thermoelectric properties of optimized InGaN

J. Appl. Phys. **110**, 123709 (2011)

A comparison of the growth modes of (100)- and (110)-oriented CrO₂ films through the calculation of surface and interface energies

J. Appl. Phys. **110**, 113910 (2011)

A strain relief mode at interface of GaSb/GaAs grown by metalorganic chemical vapor deposition

Appl. Phys. Lett. **99**, 221917 (2011)

Additional information on *Appl. Phys. Lett.*

Journal Homepage: <http://apl.aip.org/>

Journal Information: http://apl.aip.org/about/about_the_journal

Top downloads: http://apl.aip.org/features/most_downloaded

Information for Authors: <http://apl.aip.org/authors>

ADVERTISEMENT



LakeShore Model 8404 developed with **TOYO Corporation**
NEW AC/DC Hall Effect System Measure mobilities down to 0.001 cm²/V s

Epitaxial growth and demonstration of hexagonal BN/AlGaN p-n junctions for deep ultraviolet photonics

S. Majety, J. Li, X. K. Cao, R. Dahal, B. N. Pantha, J. Y. Lin, and H. X. Jiang^{a)}

Department of Electrical and Computer Engineering, Texas Tech University, Lubbock, Texas 79409, USA

(Received 16 December 2011; accepted 19 January 2012; published online 9 February 2012)

Recent advances in epitaxial growth and demonstration of p-type conductivity in hexagonal boron nitride (hBN) epilayers represent an exceptional opportunity to revolutionize p-layer approach and overcome the intrinsic problem of low p-type conductivity in Al-rich AlGaN for deep ultraviolet (DUV) device applications. Nevertheless, the ability of epitaxial growth of hBN on AlGaN is a prerequisite for the incorporation of p-type hBN in AlGaN DUV device structures. We report on the epi-growth of hBN on Al-rich AlGaN/AlN/Al₂O₃ templates using metal organic chemical vapor deposition. X-ray diffraction measurement revealed a 2θ peak at 26.5° which indicates that the BN epilayers are hexagonal and consist of a single phase. Mg doped hBN epilayers were also grown on highly insulating AlN and n-type AlGaN templates with an attempt to demonstrate hBN/AlGaN p-n junctions. Mg doped hBN epilayers grown on insulating templates were p-type with an in-plane resistivity of $\sim 2.3 \Omega \text{ cm}$. Diode behavior in the p-n structures of p-hBN/n-Al_xGa_{1-x}N ($x \sim 0.62$) has been demonstrated. The results here reveal the feasibility of using highly conductive p-type hBN as an electron blocking and p-contact layers for AlGaN deep UV emitters. © 2012 American Institute of Physics. [doi:10.1063/1.3682523]

Hexagonal boron nitride (hBN) has attracted a lot of interest recently owing to its excellent physical properties such as high thermal conductivity, chemical stability, negative electron affinity and a large energy band gap ($E_g \sim 6 \text{ eV}$).¹⁻⁵ The hexagonal structure and similar lattice constants to graphene make it highly suitable for use as a template in graphene electronics and also as a gate dielectric layer.⁶⁻⁸ Moreover, lasing action in deep ultraviolet (DUV) region ($\sim 225 \text{ nm}$) by electron beam excitation was demonstrated in small hBN bulk crystals synthesized by a high pressure/temperature technique,⁵ raising its promise as a DUV photonic material. Previous reports on the growth of hBN thin films were confined to sapphire, Ni (111) and silicon substrates.^{9,10}

On the other hand, AlGaN materials system has been the prime choice to realize solid-state DUV light sources. Due to the intrinsic problem of low p-type conductivity in AlGaN, an Al-rich AlGaN epilayer is generally used as an electron blocking layer in nearly all DUV emitters. However, the use of such a highly resistive layer in the device structure strongly affects the hole injection efficiency in the active layer.^{11,12} We have previously reported a considerable reduction in p-type resistivity of Mg doped hBN (hBN:Mg) compared to AlN:Mg ($\rho \sim 12 \Omega\text{-cm}$ for hBN:Mg vs $\rho > 10^4 \Omega\text{-cm}$ for AlN:Mg).¹³ The results suggested that it is possible to come up with a radically different DUV emitter structure which would employ p-hBN as an electron blocking layer or even p-contact layer. Highly conductive p-type hBN with its wide bandgap would effectively block the electrons and enhance the hole injection and hence the electron and hole recombination efficiency in the active region. The focus of the present work is to demonstrate the feasibility of growing hBN epilayers on AlN/Al₂O₃ and n-Al_xGa_{1-x}N/AlN/Al₂O₃ templates which would ultimately pave the way toward the

realization of high efficiency nitride DUV optoelectronic devices using this unconventional p-layer approach.

The hBN epilayers were grown using low pressure metal organic chemical vapor deposition (MOCVD). The precursors for boron and nitrogen are triethyl boron (TEB) and ammonia (NH₃), respectively. The hBN epilayers were grown on AlN and n-Al_xGa_{1-x}N ($x \sim 0.62$) templates. The $1 \mu\text{m}$ thick Si doped n-AlGaN epilayer templates were grown by MOCVD on 2-in. (0001) sapphire substrates and generally exhibit an n-type conductivity of about $0.01 \Omega \text{ cm}$. Prior to the n-AlGaN epilayer growth, a $0.5 \mu\text{m}$ undoped AlN epilayer was first deposited on sapphire substrate to serve as a template and dislocation filter.^{11,14} Figure 1 shows the schematics of the layer structures used in this study. For the growth of Mg doped hBN, biscyclopentadienyl-magnesium was transported into the reactor during hBN epilayer growth. X-ray diffraction (XRD) was used to measure the crystalline structure, quality and lattice constant of the hBN layers. Photoluminescence (PL) studies were conducted on these samples using our DUV laser spectroscopy system.¹⁵

Figure 2(a) shows the XRD θ - 2θ scan of hBN/AlN/Al₂O₃ with the hBN (002) and AlN (002) peaks placing at 26.5° and 36.0° , respectively. The (002) peak of hBN epilayer yields a corresponding lattice constant of $c = 6.70 \text{ \AA}$ which is very close to the hexagonal phase lattice constant of 6.66 \AA (Ref. 16) and the c -lattice constant (6.67 \AA) of hBN epilayers grown on sapphire substrate.¹³ No other XRD diffraction peak is observed indicating that these BN epilayers grown on AlN templates are indeed single hexagonal phase. The rocking curve of this (002) reflection, shown in Fig. 2(b), has a full width at half maximum (FWHM) of 662 arc sec which is larger than those grown on sapphire (385 arc sec) indicating that the growth conditions can be further improved.¹³

The growth is carried out under nitrogen rich condition and the variation of NH₃ exposure time did not change the

^{a)} Electronic mail: hx.jiang@ttu.edu.

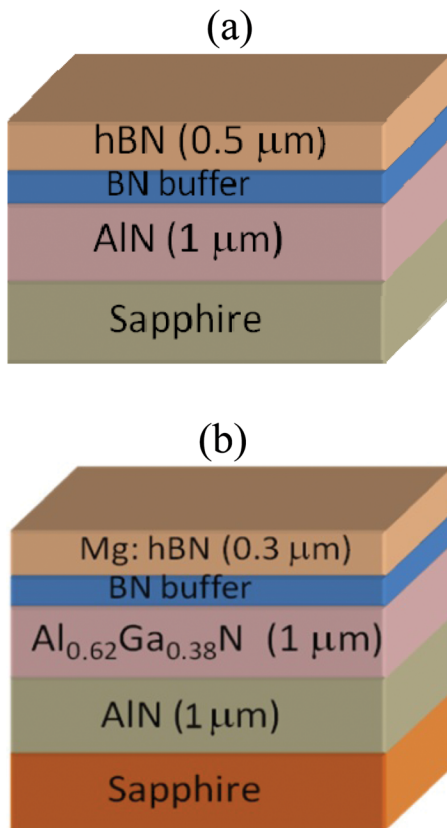


FIG. 1. (Color online) Schematic layer structures of (a) hBN/AIN/Al₂O₃ and (b) hBN:Mg/n-AlGaIn/AlN/Al₂O₃.

quality of the films, as the growth rate is independent of the NH₃ flow rate. Increase in TEB flow rate increases the growth rate and may also reduce the number of boron vacancies. Due to the large lattice mismatch between BN and AlN (in-plane lattice constants 2.5 Å and 3.1 Å, respectively), a low temperature BN buffer layer grown at 800 °C is incorporated before the growth of hBN epilayer. It has been observed that without this buffer layer, the adhesivity of hBN layers on top of the templates is compromised and the epilayer tends to peel or gets cracked very easily. We have studied the impact of this buffer layer thickness on the quality of the epilayers and have arrived at the optimum buffer layer thickness required to grow better quality hBN epilayers. The thickness of this BN buffer layer was decreased from 140 to 20 nm. An increase in XRD intensity and also a reduction in the FWHM (from 0.78° to 0.66°) of the hBN epilayers was observed as the buffer layer thickness was decreased. Table I summarizes the variation of the FWHM of the hBN (002) rocking curve with decreasing buffer thickness.

Room temperature (300 K) and low temperature (10 K) PL spectra for hBN grown on AlN/Al₂O₃ templates are shown in Fig. 3. PL spectra measured at 10 K shows a dominant emission at ~5.33 eV. Two impurity related transitions at 3.37 and 3.66 eV are also evident. The 5.33 eV transition line has been observed by several groups from hBN powder samples and pyrolytic hBN deposited by chemical vapor deposition method and thought to be related with the donor-acceptor-pair (DAP) transition. The exact natures of donor and acceptor impurities involved are however not yet clear.¹⁷

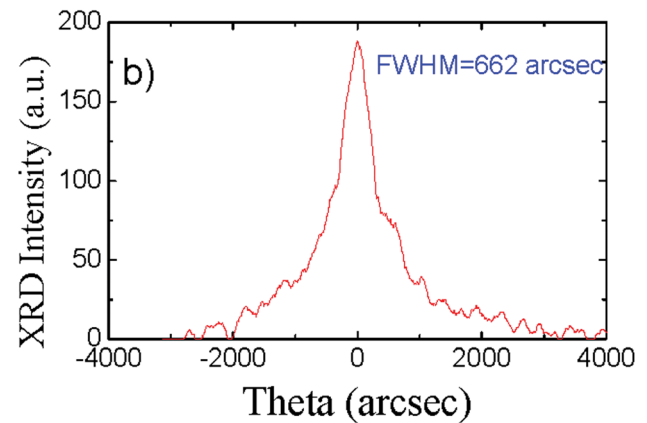
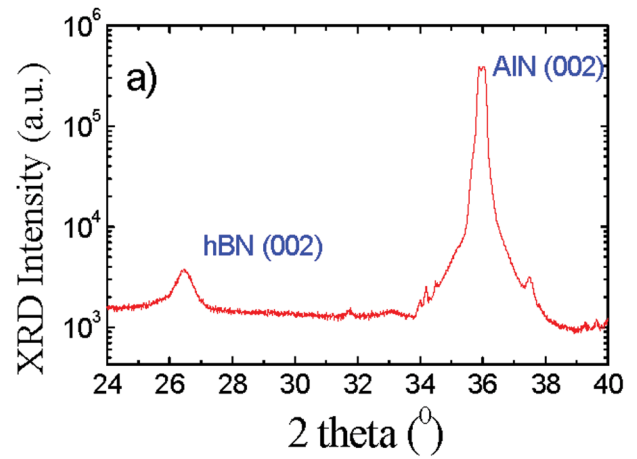


FIG. 2. (Color online) (a) XRD θ - 2θ scan of hBN/AIN/Al₂O₃ showing hBN (002) and AlN (002) peaks and (b) rocking curve of the (002) peak of hBN.

Similar to the AlGaIn materials system, post-growth thermal annealing process is generally necessary to activate Mg acceptors in Mg doped hBN epilayers. The as-grown samples were annealed at a temperature of 1150 °C for 45 min under nitrogen ambient atmosphere in order to activate the Mg acceptors. This process renders a p-type resistivity of ~2.3 Ω cm for Mg doped hBN epilayers grown on insulating templates, which has been improved by a factor of about 5 compared to our previous results for hBN:Mg/sapphire.¹³ For p-type hBN on n-Al_{0.62}Ga_{0.38}N/AlN/Al₂O₃ p-n structure, the sample was etched down to the n-Al_{0.62}Ga_{0.38}N layer using inductively coupled plasma (ICP) dry etching processing and n-contacts consisting of 30-nm-thick Ti,

TABLE I. Dependence of FWHM of (002) XRD rocking curve and c -lattice constant (c) on the thickness of the BN low temperature buffer layer (L_b).

L_b (nm)	c (Å)	FWHM (°)
140	6.77	0.78
120	6.76	1.19
100	6.76	1.00
80	6.71	0.76
60	6.76	0.78
40	6.74	0.72
30	6.74	0.81
20	6.72	0.66

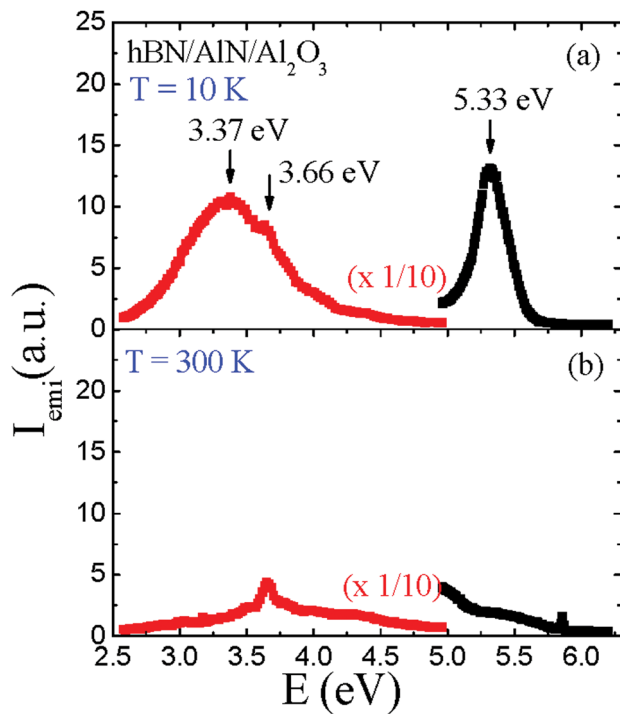


FIG. 3. (Color online) Photoluminescence spectra of hBN grown on AlN/Al₂O₃ templates measured at (a) T = 10 K and (b) T = 300 K.

100-nm-thick-Al, 30-nm-thick-Ni and 100-nm-thick-Au metal layers were deposited. The n-contacts were then subjected to thermal treatment (1050 °C for 5 s in nitrogen ambient) in order to decrease the contact resistance and enhance the ohmic behavior of these contacts.

P-contacts were formed by depositing 30-nm-thick Ni and 120-nm-thick-Au layers on the top Mg doped p-type BN. The current-voltage (I-V) characteristics of p-type hBN on n-Al_xGa_{1-x}N/AlN/Al₂O₃ p-n structure were measured at room temperature to investigate the effect of different annealing conditions on the properties of the vertical transport and ohmic contacts to p-hBN grown on n-Al_{0.62}Ga_{0.38}N/AlN/Al₂O₃ templates. The I-V characteristics with different annealing conditions are shown in Fig. 4, which shows that thermal annealing of the contacts is critical and annealing under N₂ ambient above 920 °C for 2 min provides good ohmic contacts. We have noticed that at a temperature greater than 1000 °C the Ni/Au contacts fuse together to form an alloy and tend to get detached from the Mg doped p-type BN layer. However with just the 30 nm Ni layer without Au, annealing at 1020 °C for 1 min makes the contact ohmic and the contact resistance is drastically reduced.

In addition to the need of thermal annealing treatment of the p-contacts, we also found that doping the buffer layer with Mg significantly improves the vertical transport properties. Figure 5 shows the I-V characteristics and schematic illustration of a p-n structure in which the buffer layer was doped with Mg and p-contacts were annealed at 1020 °C. As can be seen from Fig. 5, we were able to demonstrate a decent diode behavior in hBN:Mg/n-AlGaN. The leakage current under reverse bias can be controlled to be quite low (~3 μA at -10 V). This approach has the potential to solve the problem of low quantum efficiency of DUV devices

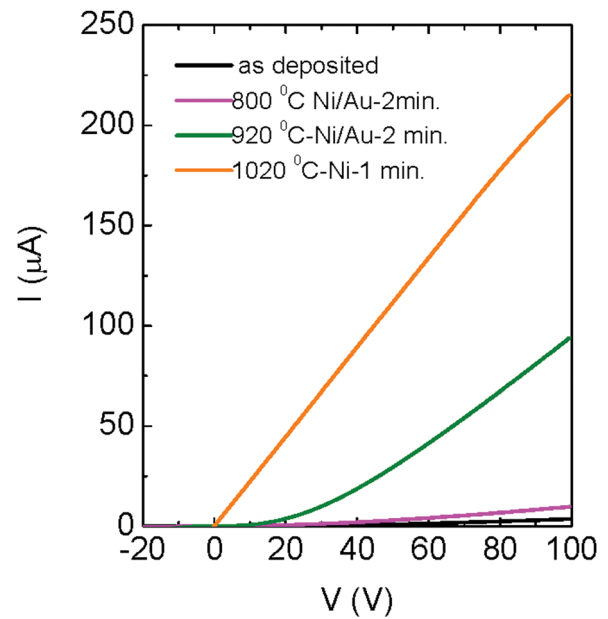


FIG. 4. (Color online) I-V characteristics of the Mg doped p-type hBN epilayers deposited on Si-doped n-AlGa_{1-x}N with Ni/Au and Ni contacts annealed at different times and temperatures.

using Al-rich AlGa_{1-x}N alloys due to their extremely low p-type conductivity.

In summary, we have demonstrated epitaxial growth of hBN on III-nitride templates. Diode structures consisting of p-hBN on n-Al_xGa_{1-x}N were fabricated and their I-V characteristics were measured. Thermal annealing of the p-contacts was performed to study the effects of different annealing conditions. The p-hBN/n-AlGa_{1-x}N heterostructures revealed a diode behavior with a current of ~7.5 mA at a

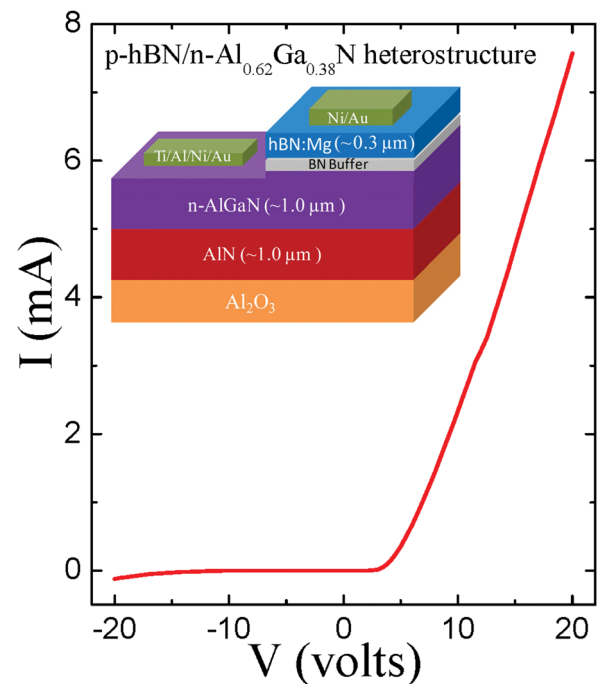


FIG. 5. (Color online) I-V characteristics of a p-hBN:Mg/n-Al_{0.62}Ga_{0.38}N/AlN structure with p-contacts annealed at 1020 °C exhibiting a diode behavior. The inset shows the schematic diagram of the p-n structure, in which BN buffer layer is doped with Mg.

bias voltage of 20 V. Further improvements in material quality, p-type conductivity, the type of ohmic contacts, and post-growth processes would enhance the properties of these p-n structures which could ultimately pave the way toward the realization of high efficiency nitride DUV optoelectronic devices.

This work is supported by DARPA-CMUVT program (grant #FA2386-10-1-4165 managed by Dr. John Albrecht). The hBN epi-growth effort is also supported in part by DHS ARI Program (grant #2011-DN-077-ARI 048-02 managed by Dr. Mark Wrobel). Jiang and Lin are grateful to the AT&T Foundation for the support of Ed Whitacre and Linda Whitacre endowed chairs and to Dr. Mike Wraback of Army Research Laboratory for insightful discussion.

¹Y. Kubota, K. Watanabe, O. Tsuda, and T. Taniguchi, *Science* **317**, 932 (2007).

²T. Sugino, C. Kimura, and T. Yamamoto, *Appl. Phys. Lett.* **80**, 3602 (2002).

³D. Pacilé, J. C. Meyer, Ç. Ö. Girit, and A. Zettl, *Appl. Phys. Lett.* **92**, 133107 (2008).

⁴L. Song, L. Ci, H. Lu, P. B. Sorokin, C. Jin, J. Ni, A. G. Kvashnin, D. G. Kvashnin, J. Lou, B. I. Yakobson *et al.*, *Nano Lett.* **10**, 3209 (2010).

⁵K. Watanabe, T. Taniguchi, and H. Kanda, *Nat. Photonics* **3**, 591 (2009).

⁶Y. Shi, C. Hamsen, X. Jia, K. K. Kim, A. Reina, M. Hofmann, A. L. Hsu, K. Zhang, H. Li, Z. Juang *et al.*, *Nano Lett.* **10**, 4134 (2010).

⁷N. Alem, R. Erni, C. Kisielowski, M. D. Rossell, W. Gannett, and A. Zettl, *Phys. Rev. B* **80**, 155425 (2009).

⁸C. R. Dean, A. F. Young, I. Meric, C. Lee, L. Wang, S. Sorgenfrei, K. Watanabe, T. Taniguchi, P. Kim, K. L. Shepard *et al.*, *Nat. Nanotechnol.* **5**, 722 (2010).

⁹Y. Kobayashi, T. Nakamura, T. Akasaka, T. Makimoto, and N. Matsumoto, *J. Cryst. Growth* **298**, 325 (2007).

¹⁰Y. Kobayashi and T. Akasaka, *J. Cryst. Growth* **310**, 5044 (2008).

¹¹M. L. Nakarmi, K. H. Kim, M. Khizar, Z. Y. Fan, J. Y. Lin, and H. X. Jiang, *Appl. Phys. Lett.* **86**, 092108 (2005).

¹²C. Pernot, M. Kim, S. Fukahori, T. Inazu, T. Fujita, Y. Nagasawa, A. Hirano, M. Ippommatsu, M. Iwaya, S. Kamiyama *et al.*, *Appl. Phys. Express* **3**, 061004 (2010).

¹³R. Dahal, J. Li, S. Majety, B. N. Pantha, X. K. Cao, J. Y. Lin, and H. X. Jiang, *Appl. Phys. Lett.* **98**, 211110 (2011).

¹⁴M. L. Nakarmi, K. H. Kim, K. Zhu, J. Y. Lin, and H. X. Jiang, *Appl. Phys. Lett.* **85**, 3769 (2004).

¹⁵K. B. Nam, M. L. Nakarmi, J. Y. Lin, and H. X. Jiang, *Appl. Phys. Lett.* **86**, 222108 (2005).

¹⁶R. S. Pease, *Acta Crystallogr.* **5**, 356 (1952).

¹⁷L. Museur and A. Kanaev, *J. Appl. Phys.* **103**, 103520 (2008).